



Review

Translating Research for the Radiotheranostics of Nanotargeted ^{188}Re -Liposome

Chih-Hsien Chang ^{1,2,*}, Ming-Cheng Chang ¹, Ya-Jen Chang ¹, Liang-Cheng Chen ¹, Te-Wei Lee ¹ and Gann Ting ¹

¹ Isotope Application Division, Institute of Nuclear Energy Research, Taoyuan 32546, Taiwan; mcchang@iner.gov.tw (M.-C.C.); yjchang@iner.gov.tw (Y.-J.C.); lcchen@iner.gov.tw (L.-C.C.); tewei123456@gmail.com (T.-W.L.); gann.ting@msa.hinet.net (G.T.)

² Department of Biomedical Imaging and Radiological Sciences, National Yang Ming Chiao Tung University, Taipei 11221, Taiwan

* Correspondence: chchang@iner.gov.tw

Abstract: Nanoliposomes are one of the leading potential nano drug delivery systems capable of targeting chemotherapeutics to tumor sites because of their passive nano-targeting capability through the enhanced permeability and retention (EPR) effect for cancer patients. Recent advances in nano-delivery systems have inspired the development of a wide range of nanotargeted materials and strategies for applications in preclinical and clinical usage in the cancer field. Nanotargeted ^{188}Re -liposome is a unique internal passive radiotheranostic agent for nuclear imaging and radiotherapeutic applications in various types of cancer. This article reviews and summarizes our multi-institute, multidiscipline, and multi-functional studied results and achievements in the research and development of nanotargeted ^{188}Re -liposome from preclinical cells and animal models to translational clinical investigations, including radionuclide nanoliposome formulation, targeted nuclear imaging, biodistribution, pharmacokinetics, radiation dosimetry, radiation tumor killing effects in animal models, nanotargeted radionuclide and radio/chemo-combination therapeutic effects, and acute toxicity in various tumor animal models. The systemic preclinical and clinical studied results suggest ^{188}Re -liposome is feasible and promising for in vivo passive nanotargeted radionuclide theranostics in future cancer care applications.

Keywords: liposome; nanoliposome; nuclear imaging; radiotheranostics; rhenium-188



Citation: Chang, C.-H.; Chang, M.-C.; Chang, Y.-J.; Chen, L.-C.; Lee, T.-W.; Ting, G. Translating Research for the Radiotheranostics of Nanotargeted ^{188}Re -Liposome. *Int. J. Mol. Sci.* **2021**, *22*, 3868. <https://doi.org/10.3390/ijms22083868>

Academic Editor: Agnes Csiszár

Received: 18 March 2021

Accepted: 30 March 2021

Published: 8 April 2021

Publisher's Note: MDPI stays neutral with regard to jurisdictional claims in published maps and institutional affiliations.



Copyright: © 2021 by the authors. Licensee MDPI, Basel, Switzerland. This article is an open access article distributed under the terms and conditions of the Creative Commons Attribution (CC BY) license (<https://creativecommons.org/licenses/by/4.0/>).

1. Introduction

Over the past few decades, theranostics has emerged as a field in which diagnosis and targeted therapy are combined to achieve a personalized treatment approach to the patient [1]. The progress in molecular biology and the understanding of malignant transformation and tumorigenesis have revealed recognition of the widespread applicability of the hallmarks of cancer concepts. These novel concepts increasingly affect the development of new means to treat human cancer in personalized and translational medicine. Conventionally, anticancer drugs are used to systemically destroy any residual or metastatic tumor cells, but they cannot discriminate between neoplastic and non-neoplastic cells [2]. Besides, poor solubility and distribution, unfavorable pharmacokinetics, and high-tissue damage or toxicity are also noted in various therapeutic agents. Therefore, an effective therapeutic strategy targeting specific mechanisms involved in tumorigenesis is needed [3]. The biggest challenges in cancer diagnostics and therapeutic radionuclide agents in clinical applications include low drug bioavailability within cancer cells and the high toxicities to normal organs [4]. An ideal delivery system can carry radionuclides into the cancer targeting area and releases the desired cytotoxic concentration at the right time. The importance of nanotechnology to radionuclide delivery systems in molecular imaging and targeted radiotherapy has been recognized this decade [5–7]. Several innovative radionuclides and drug delivery systems focused on cancer nanotechnology have been developed in recent

investigations. Liposomes have been applied to improve the targeting of radionuclide transport into tumor lesions [4,8–12]. Besides, nanotargeting delivery systems have also been revealed to reduce radionuclide cytotoxic agent side-effects.

Liposome is one of nanomedicine formulations originally designed to improve the distribution and target site accumulation of systemically administered therapeutic agents [4,12]. They are spherical, self-closed formed lipid bilayers with phospholipids in which they are entrapped radionuclides [7]. These nanosized drug delivery systems are popularly used because of increased absorption, delayed excretion, decreased uptake and removal from circulation by the reticuloendothelial system, longer half-life within the blood circulation and lower toxicity. Besides, liposomes can accumulate in tumors through leaky tumor vasculature and the enhanced permeability and retention (EPR) effect [2,13]. With these outstanding properties, liposomes have been used as targeted drug delivery systems. Recent liposome concomitant imaging radionuclides and therapeutics have drawn attention to an approach combining diagnostics and treatment in various studies [8,14,15]. Successfully combining molecular imaging and nanomedicine approaches has fundamentally contributed to a new and highly interdisciplinary research field. Harrington and his colleague reported the biodistribution and imaging of ^{111}In -diethylenetriaminepentaacetic acid (DTPA)-labeled PEGylated (polyethylene glycol, PEG) liposomes in advanced cancer patients. Tumor images from various cancer types including the breast, head and neck, bronchus, glioma and cervix were obtained by gamma camera and single photon emission computed tomography/X-ray Computed Tomography (SPECT/CT) [16]. Recently, with improvements in radiolabeling methodologies development [17], PEGylated technology [18], scanner technology and imaging quality, the liposomes in cancer diagnosis and therapy can be potentially used in clinical applications. The ^{186}Re -liposome was developed by a remote-loading method for ^{186}Re encapsulated in liposome [19]. Liposomes in the 100-nanometer size range have been the most investigated carrier for convection enhanced delivery (CED) drug delivery to the brain. They have been utilized as a carrier for radiotherapeutic rhenium-186 radionuclides to very high levels of specific activity for treating glioblastoma [9]. The phase I/II clinical studies including maximum tolerated dose (MTD), safety and efficacy of rhenium nanoliposomes in recurrent glioma of ^{186}Re -liposome (ReSPECTTM) have been promoted in the United States by Plus Therapeutics, Inc. The development of personalized theranostic radiopharmaceuticals show greater accuracy in selecting patients who may respond to treatment and allow for the assessment of the therapeutic response [7]. Rhenium (Re) and technetium (Tc) belong to the manganese family (VIIB). The chemical properties of ^{188}Re and $^{99\text{m}}\text{Tc}$ are highly similar to each other. With the readily detectable gamma ray properties and short physical/biological half-life, $^{99\text{m}}\text{Tc}$ has become the one of the most widely used radioisotopes for radiopharmaceuticals. The major advantage of ^{188}Re over other radionuclides in internal radiotherapy application is the availability and cost-effectiveness of the $^{188}\text{W}/^{188}\text{Re}$ -generator ($T_{1/2} = 69.4$ days), which has a longer shelf-life and a higher specific activity. This is convenient to use and easier to continuously supply to remote areas of the world. There are two major advantages of ^{188}Re over other radionuclides in radio-theranostic application. One is the radio-therapeutic effect of ^{188}Re derives from the high energy $E_{\beta(\text{max})}$ value of 2.12 MeV (71.1%), allowing a maximum tissue penetration range $R_{\beta(\text{max})}$ of 10.4 mm. The other is the 155-keV (15.6%) gamma ray with a half-life of 16.7 h allows tumor targeting to be monitored using gamma ray nuclear imaging.

Ionizing radiation therapy is used as a primary treatment for many types of cancer. Since 1990, radiation-induced apoptosis has been observed in several animal tumors and in different cell lines, and many investigators have identified molecular signals that control the induction of programmed cell death (apoptosis) in cells exposed to radiation [20]. Although apoptosis pathways induced by ^{188}Re beta-irradiation have been reported [21], the molecular mechanism is still an unmet need. We demonstrated the colon tumors from treated mice had a 26-fold increase in the numbers of apoptotic cells compared with those from the normal saline control mice at 8 h after treatment with ^{188}Re -liposome [22]. ^{188}Re -liposome

significantly reactivated the p53 pathway, suppressing the epithelial-to-mesenchymal transition (EMT) process [23,24] and the reversal of glycolysis in an ovarian tumor model [23]. ^{188}Re -liposome also effectively suppressed the expression of stemness-relevant markers of cancer-stem cells and may be a novel treatment for ovarian cancer when delivered intraperitoneally [23]. In addition, ^{188}Re -liposome could induce the autophagy/mitophagy of cancer stem cells, leading to tumor regression in the ovarian tumor animal model [25].

MicroRNA, an abundant family of short (19–25 nucleotides) noncoding RNAs, can modulate gene expression upon binding to target mRNAs. The aberrant expression of miRNAs can regulate diverse cellular processes, including the apoptosis of tumor cells [26]. Microarray analysis revealed the tumor suppressor microRNA let-7 could be induced by ^{188}Re -liposome to regulate downstream genes in human head and neck squamous cell carcinoma (HNSCC) [27]. Most ^{188}Re -liposome that up-regulate microRNAs, including miR-206-3p, were categorized as tumor suppressors, while down-regulate microRNAs, including miR-142-5P, were oncogenic [28]. Studies on the regulation of microRNAs correlate to the therapeutic efficacy of ^{188}Re -liposome in HNSCC tumor [27,28]. The evidence indicated ^{188}Re -liposome enhances various anti-tumor mechanisms in tumor therapy. Figure 1 overviews the possible mechanisms in the anticancer effects of ^{188}Re -liposome.

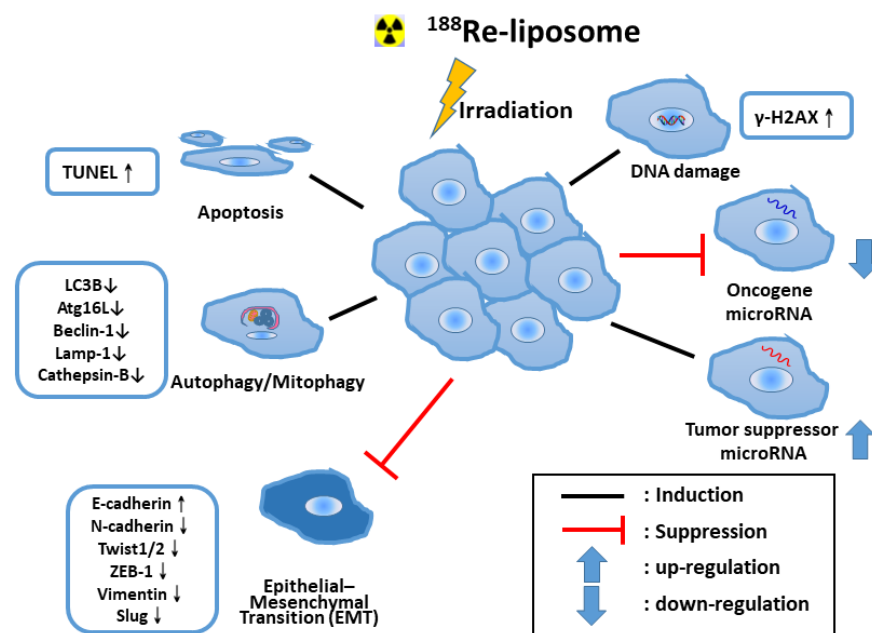


Figure 1. An overview of radiation killing mechanisms of preclinical tumor animal models in internal radiotherapy of nanotargeted ^{188}Re -liposome. TUNEL: Terminal deoxynucleotidyl transferase dUTP nick end labeling.

Our preclinical cell and animal model investigations demonstrated the efficacy and safety of nanotargeted radiotheranostic ^{188}Re -liposome or radio/chemotheranostic ^{188}Re -doxorubicin (DXR)-liposome, which includes tumor site targeting and nuclear imaging, pharmacokinetics, biodistribution, dosimetry, the radiation killing effect, and synergistic radio/chemo-combination effects. We also completed a phase 0 clinical trial for 12 patients, which showed the potential of ^{188}Re -liposome as a new nanotargeted anti-cancer radiotherapeutic [29]. The current review and summaries focus on the systemic overview and comparisons of our preclinical nanotargeted ^{188}Re -liposome pharmacology, therapeutic effects, and safety studies in animal models, leading to translational clinical investigations' achievements (Table 1) and promoting the advancement and utilization of nanotargeted ^{188}Re -liposome in future cancer clinical research and practical applications.

Table 1. Summary of preclinical and clinical studies of radio-nanotargeted ¹⁸⁸Re-(DXR)-liposome.

Preclinical Pharmacology, Therapeutic Effects and Safety Studies				
No	Animal Model	Application	Main Research	Ref
1	C26 murine colon carcinoma	Diagnosis	Solid tumor, drug stability, imaging, PK, Bio-D	[30]
2	HT-29 human colorectal adenocarcinoma	Diagnosis	Solid tumor, drug stability, imaging, PK, Bio-D, T/N ratio, autoradiogram	[31]
3	C26 murine colon carcinoma	Diagnosis	Ascites meta, drug stability imaging, PK, Bio-D, autoradiogram	[32]
4	F98 rat brain glioma	Diagnosis	Solid tumor, drug stability, imaging, PK, Bio-D, high T/N ratio, autoradiogram	[33]
5	C26 murine colon carcinoma	Therapy	Solid tumor, PK, Bio-D, comparison ¹⁸⁸ Re-liposome/Lipo-DOX, synergistic therapy effect of ¹⁸⁸ Re-DXR-liposome, histology	[34]
6	C26 murine colon carcinoma	Therapy	Solid tumor, comparison ¹⁸⁸ Re-liposome/5-FU, safety, radiation effect	[22]
7	C26 murine colon carcinoma	Therapy	Ascites meta, Imaging, PK, Bio-D, autoradiogram, comparison ¹⁸⁸ Re-liposome/Lipo-DOX, synergistic therapy effect of ¹⁸⁸ Re-DXR-liposome, histology	[35]
8	C26 murine colon carcinoma	Therapy	Ascites meta, Imaging, PK, Bio-D, dosimetry, comparison ¹⁸⁸ Re-liposome/5-FU	[36]
9	C26 murine colon carcinoma	Therapy	Lung meta, PK, Bio-D, dosimetry, excretion, comparison ¹⁸⁸ Re-liposome/5-FU	[37]
10	LS-174T human colon adenocarcinoma	Therapy	Solid tumor, imaging, PK, Bio-D, dosimetry, comparison ¹⁸⁸ Re-liposome/5-FU	[38]
11	4T1 murine breast cancer	Therapy	Orthotopic tumor, imaging, Bio-D, comparison ¹⁸⁸ Re-liposome/Lipo-DOX	[39]
12	NCI-H292 non-small cell lung cancer	Therapy	Solid tumor, imaging, Bio-D, PK, comparison ¹⁸⁸ Re-liposome/ ¹⁸⁸ Re-BMEDA	[40]
13	FaDu human hypopharyngeal carcinoma	Therapy	Orthotopic meta, imaging, Bio-D, PK, comparison ¹⁸⁸ Re-liposome/ ¹⁸⁸ Re-BMEDA	[27]
14	ES-2-luc human ovarian cancer	Therapy	Ascites meta, imaging, comparison ¹⁸⁸ Re-liposome/ ¹⁸⁸ Re-BMEDA, radiation effect	[23]
15	F98 rat brain glioma	Therapy	Solid tumor, dosimetry, histology, comparison ¹⁸⁸ Re-liposome/ ¹⁸⁸ Re-BMEDA	[41]
16	C26 murine colon carcinoma	Therapy	Liver meta, imaging, combination of ¹⁸⁸ Re-liposome/Nexavar	[42]
17	C26 murine colon carcinoma	Therapy	Solid tumor, Bio-D, PK, combination of ¹⁸⁸ Re-liposome/Lipo-Dox	[43]
18	BE-3 human esophageal adenocarcinoma	Therapy	Solid tumor, imaging, Bio-D, safety, combination of ¹⁸⁸ Re-liposome/EBRT	[44]
19	Acute toxicity of BMEDA in ICR mice	Safety	No Observed Adverse Effect Level (3 mg/kg)	[45]
20	Acute toxicity of BMEDA in Beagle dog	Safety	No Observed Adverse Effect Level (2 mg/kg)	[46]
21	Extended acute toxicity of ¹⁸⁸ Re-liposome in SD rat	Safety	No Observed Adverse Effect Level (185 MBq/kg)	[47,48]
Clinical Safety and Therapeutic Effects Studies				
1	Phase 0 eIND-metastatic tumors, 12 patients	Safety	Imaging, safety, dosimetry	[29]
2	Low dose clinical trial for 2 ovarian cancer patients	Therapy	Safety, preliminary therapy evaluation, radiation effect	[25]

Bio-D: Biodistribution; BMEDA: *N,N*-bis(2-mercaptoethyl)-*N',N'*-diethyl-ethylenediamine; DXR: doxorubicin; EBRT: External beam radiotherapy; eIND: exploratory Investigational New Drug; ICR mice: Institute of Cancer Research mice; PK: Pharmacokinetics; SD rat: Sprague Dawley rat; T/N ratio: Tumor/Non-tumor ratio.

2. Rhenium-188 Production

The most important achievement in using ^{188}Re is the development of a $^{188}\text{W}/^{188}\text{Re}$ -generator. The $^{188}\text{W}/^{188}\text{Re}$ -generator is easy to manipulate and practical, especially in some remote areas where it is difficult to transport short-living radionuclides routinely. Originally, ^{188}W is produced by the $^{186}\text{W}(2n,\gamma)^{188}\text{W}$ nuclear reaction [49,50]. This reaction involves two successive neutron captures, making the probability of a reaction proportional to the square of the neutron flux. Consequently, the production depends on the neutron flux. However, only very high neutron flux ($10^{15}/\text{cm}^2/\text{second}$) can produce sufficient ^{188}W . Currently, a $^{188}\text{W}/^{188}\text{Re}$ -generator design is based on ^{188}Re separation from ^{188}W using an alumina column. For instance, the parent nuclide, ^{188}W , is loaded on the column and a ^{188}Re daughter radionuclide is eluted with normal saline. The half-life of ^{188}W is 69 days. Therefore, the shelf life of an $^{188}\text{W}/^{188}\text{Re}$ -generator can be longer than four months, based on the activity levels of ^{188}Re required. The interval of ^{188}Re elution to achieve the maximum radioactivity is approximately three days [51]. For the preparation of ^{188}Re -liposome, ^{188}Re could be milked from a homemade $^{188}\text{W}/^{188}\text{Re}$ -generator of the Institute of Nuclear Energy Research [52] or a commercialized Good Manufacturing Practice (GMP)/Pharmaceutical-Grade $^{188}\text{W}/^{188}\text{Re}$ generator by IRE (Institut National des Radioelements, Fleurus, Belgium).

3. Preparation and Characterization of ^{188}Re -Liposome

^{188}Re -liposome is composed of liposome (Carrier), *N,N*-bis(2-mercaptoethyl)-*N',N'*-diethyl-ethylenediamine (BMEDA, chelator) and ^{188}Re (Radionuclide) by a remote-loading method [19]. BMEDA is a nitrogen and sulfur donor (SNS) pattern ligand with a tridentate structure that has one nitrogen and two sulfur atoms (Figure 2A). These three atoms are able to offer electrons to ^{186}Re , ^{188}Re and ^{99}Tc for organizing a lipophilic complex in a neutral state [19] (Figure 2B). The SNS/S complexes have a neutral core coordinate structure which can cross the lipophilic double membrane of a liposome. Carrier-free ^{188}Re -perrhenate (NaReO_4) and BMEDA were used to form ^{188}Re -BMEDA [9]. The labeling efficiency of ^{188}Re -BMEDA is usually more than 95%. Liposomes encapsulating $(\text{NH}_4)_2\text{SO}_4$ have been chosen as the drug delivery scaffold [9]. With ^{188}Re -BMEDA crossing the lipophilic bilayer of liposome, the lipophilic/hydrophilic characterization can trigger a gel-like formation and anions trapping (Figure 2C). The ^{188}Re -liposome was separated from free ^{188}Re -BMEDA using a PD-10 column eluted with normal saline. The overall yield of ^{188}Re -liposome is about 70%. For clinical trials, ^{188}Re -liposome was further filtered with a 0.22 micrometer filter in our Pharmaceutical Inspection Convention and Pharmaceutical Inspection Cooperation Scheme (PIC/S) GMP radiopharmaceutical production center. The specification for the concentration of phospholipid were 3~6 $\mu\text{mol}/\text{mL}$, a particle size of 80~100 nm, zeta potential of -3~2 mV and radiochemical purity of more than 90%. Figure 3 shows the scheme for the preparation of ^{188}Re -liposomes [32]. Studies have indicated ^{188}Re -liposome is stable in normal saline, serum and plasma [30,32,53]. The results from in vitro and in vivo studies indicated that about 92~98% of ^{188}Re -liposomes maintain high radiochemical purity (RCP) for up to 72 h of incubation [30-32,53]. The evidence indicates ^{188}Re -liposome has high radiochemical purity and drug encapsulation stability.

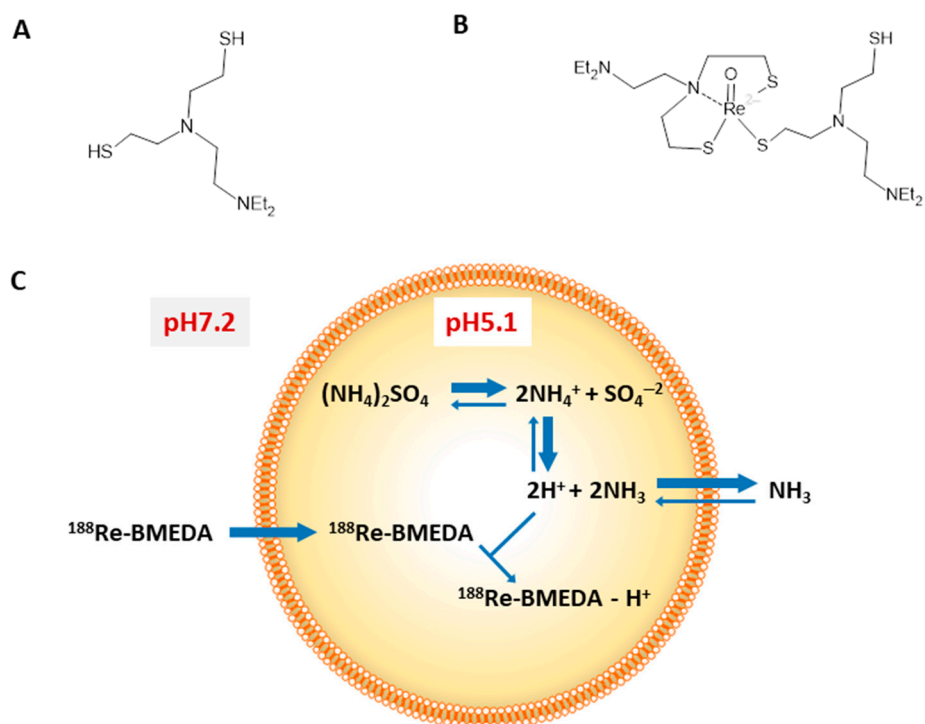


Figure 2. Chemical structure of BMEDA (A) and ^{188}Re -BMEDA (B). Diagram (C) depicting after-loading method for liposomes containing ammonium sulfate pH gradient radiolabeled with ^{188}Re -BMEDA. The lipophilic form of BMEDA at pH 7.2 crosses the lipid bilayer. Once inside the liposome interior, BMEDA becomes protonated at pH 5.1 and trapped within the hydrophilic liposome interior as ^{188}Re -BMEDA- H^+ form. This research was originally published in JNM [19].

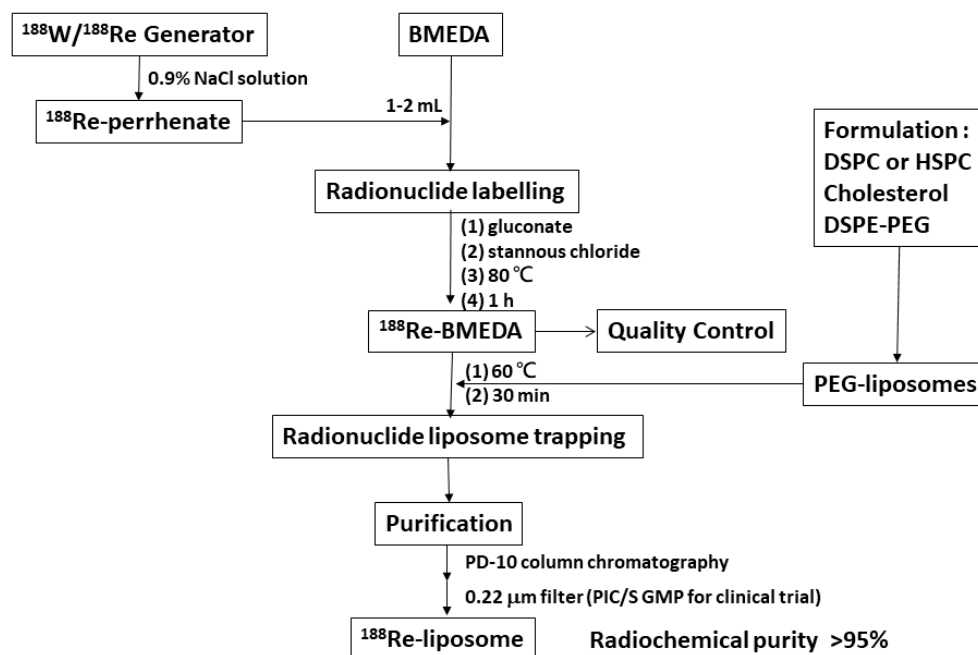


Figure 3. Chemical flowsheet for the preparation of ^{188}Re -liposomes. DSPC: 1,2-Distearoyl-sn-Glycero-3-Phosphocholine; HSPC: Hydrogen Soybean Phosphotidylcholine. Figure adapted with permission from [32].

4. Preclinical Studies of ^{188}Re -Liposome

4.1. Pharmacokinetics and Biodistribution

For pharmacokinetics, whole blood samples were collected for up to 168 h (lung metastatic model up to 96 h) post administration through the tail vein. Radioactivity in whole blood samples was normalized to the percentage of injected dose per gram at various time points following the intravenous injection of ^{188}Re -liposome. Pharmacokinetic parameters were determined using the WinNonlin software v5.0.1 (Pharsight Corp., Mountain View, CA, USA). Non-compartmental analysis was used with the log/linear trapezoidal rule. The pharmacokinetic parameters, including time to achieve maximum concentration (T_{max}), maximum concentration (C_{max}), clearance (Cl), area under the tissue concentration–time curve (AUC), and mean residence time (MRT) were determined. Pharmacokinetic parameters of ^{188}Re -liposome from blood in various cancer-bearing mice models have been estimated [30,32,36,37]. The elimination half-life ($T_{1/2\lambda_z}$) of ^{188}Re -liposome and ^{188}Re -BMEDA was 185.33 h and 34.72 h, respectively, in a C26 ascites tumor model [32]. $T_{1/2\lambda_z}$ of ^{188}Re -liposome was 5.3-fold longer than that of ^{188}Re -BMEDA in blood. The $\text{AUC}_{(0\rightarrow\infty)}$ of ^{188}Re -liposome and ^{188}Re -BMEDA was 763.03% ID/g \times h and 81.28% ID/g \times h, respectively. The $\text{AUC}_{(0\rightarrow\infty)}$ of ^{188}Re -liposome in blood was 9.4-fold larger than that of ^{188}Re -BMEDA. The total body clearance of ^{188}Re -BMEDA (1.23 mL/h) was higher than that of ^{188}Re -liposome (0.13 mL/h). Furthermore, The $\text{AUC}_{(0\rightarrow\infty)}$ of ^{188}Re -liposome and ^{188}Re -BMEDA was 800.6% ID/g \times h and 172.6% ID/g \times h, respectively, in a C26 solid tumor model [30]. The $\text{AUC}_{(0\rightarrow\infty)}$ of ^{188}Re -liposome in blood was 4.65-fold larger than that of ^{188}Re -BMEDA. The $\text{AUC}_{(0\rightarrow\infty)}$ of ^{188}Re -liposome and ^{188}Re -BMEDA was 488.97% ID/g \times h and 62.73% ID/g \times h, respectively, in an NCI-H292 solid tumor model [40]. The $\text{AUC}_{(0\rightarrow\infty)}$ of ^{188}Re -liposome in blood was 7.8-fold larger than that of ^{188}Re -BMEDA. These pharmacokinetic parameters indicate ^{188}Re -liposome has significantly greater MRT with longer $T_{1/2\lambda_z}$ and the greater AUC compared with those from ^{188}Re -BMEDA.

All biodistribution showed ^{188}Re -liposome could accumulate significant amounts in the tumor, liver, spleen and kidneys [30,32,36,40,54]. Liposome could be captured in the liver and spleen by the reticuloendothelial system [2]. The highest uptake of ^{188}Re -liposome in tumors was found at 24 h after administration, and was steadily maintained until 72 h after administration. The highest tumor to muscle ratio (Tu/Mu) was up to 25.8 and 14.4 at 24 h in the C26 murine colon ascites model [36] and HT-29 human colorectal carcinoma solid tumor model [31], respectively. Very low uptake of ^{188}Re -liposome has been reported in the organs of the central nervous and musculoskeletal systems [30,36]. Biodistribution studies suggested that ^{188}Re -liposome exhibits high retention in blood circulation and tumor accumulation in vivo. Our study also showed ^{188}Re -liposome could accumulate in brain tumors. The mechanism may be due to the neoangiogenesis properties of glioma, with newly formed vasculatures overpassing the blood–brain barrier (BBB). Besides, glioma cells can degrade tight junctions by secreting soluble factors, leading to BBB disruption [33]. The excretion of ^{188}Re -liposome has been studied [36,37]. The fraction of ^{188}Re -liposome excreted in the urinary and gastrointestinal tract is derived from accumulative urine and feces using metabolic cages [37,55]. The total excreted fraction of ^{188}Re -liposome by urine and feces was about 47–87% in different tumor models. The ^{188}Re -liposome was mostly excreted via feces (29–61%), suggesting the importance of hepatobiliary excretion for these compounds.

4.2. Longitudinal MicroSPECT/CT Imaging of Tumor Targeting for ^{188}Re -Liposome

Several tumor-bearing mouse models demonstrated longitudinal microSPECT/CT could be used as the imaging of tumor targeting by using ^{188}Re -liposome [30,32,34,35,38]. The accumulation and localization of nanotargeted ^{188}Re -liposomes has been studied in C26 solid mouse models [30,34]. The images revealed ^{188}Re -liposomes (Figure 4B) and ^{188}Re -DXR-liposomes (Figure 4C) remained in the tumor for up to 72 h post injection, while the corresponding images for free ^{188}Re -BMEDA revealed it could not accumulate

in the tumor at 4 h post injection (Figure 4A). Although uptake of ^{188}Re -liposome in the spleen and liver are the common features of nanoparticles following intravenous injection into mice, the images revealed a higher uptake in tumors up to 72 h after intravenous injection. A positive correlation ($r = 0.663$) of tumor uptake of ^{188}Re -liposome by biodistribution and microSPECT semi-quantification image analysis was obtained using Pearson correlation analysis (Figure 4D) [30]. MicroSPECT/CT imaging also revealed a higher uptake of ^{188}Re -liposome in tumors up to 72 h post injection in a human LS-174T-colorectal cancer tumor-bearing mice model [38]. Whole-body autoradiography results also confirmed the correlation between microSPECT/CT imaging and biodistribution data [38]. Our results indicated molecular imaging is a non-invasive imaging modality that can longitudinally monitor the behavior of ^{188}Re -liposome radiotherapeutics in the same animal across different time points.

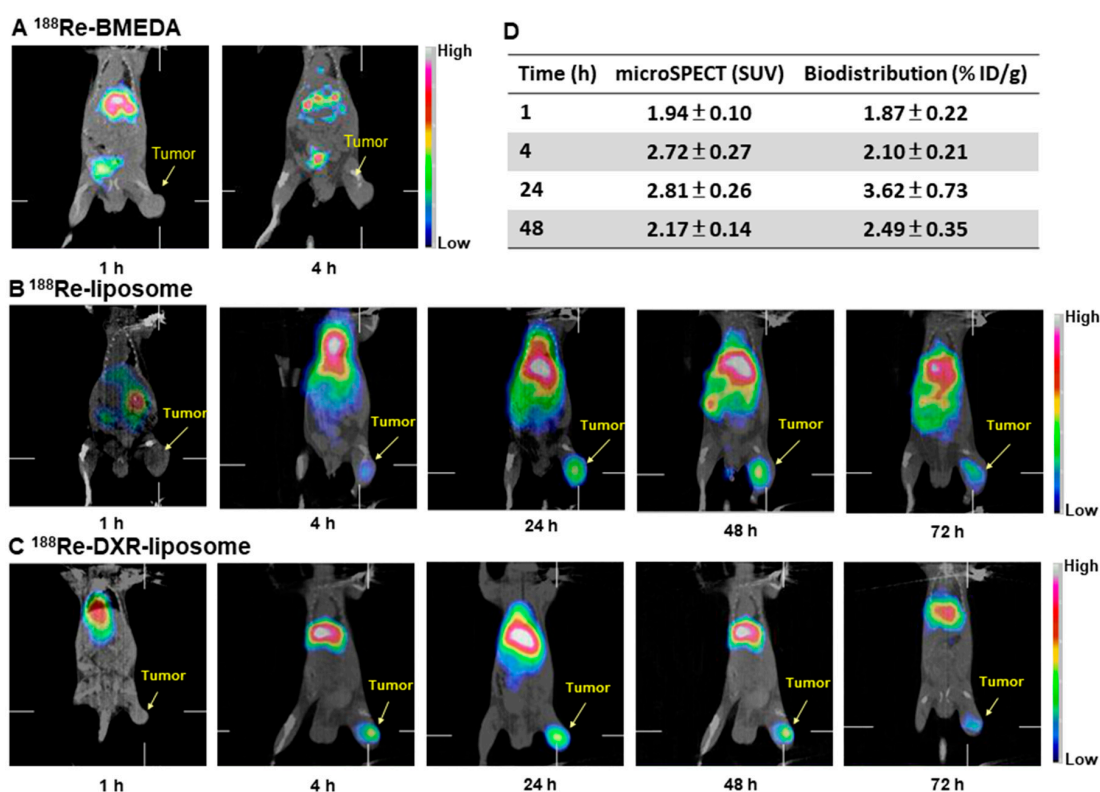


Figure 4. Micro-SPECT/CT imaging of ^{188}Re -BMEDA (A), ^{188}Re -liposome (B) and ^{188}Re -DXR-liposome (C) in C26 tumor-bearing mice. (D) Correlation of tumor uptake ^{188}Re -liposome analyzed by microSPECT imaging and biodistribution. Arrows indicate positions of subcutaneous tumors. Figures adapted with permission from [30,34].

4.3. Dosimetry of ^{188}Re -Liposome

Radiation dosimetry analysis is an important aspect of evaluating the safety and efficacy of internal emitters for radionuclide therapy [56]. Regulatory agencies (e.g., the US Food and Drug Administration, FDA) approved the use of animal models to estimate the dosimetry before clinical trials [57]. Radiation dosimetry was conducted to estimate the absorbed doses in non-target organs, as well as in target tumors for ^{188}Re -liposome, to extrapolate the animal data to humans. Radiation dose estimates for normal tissues and tumors were calculated using the OLINDA/EXM program [58].

Various studies from colon carcinoma tumor-bearing mice models indicate the absorbed dose of ^{188}Re -liposome in liver, kidneys and red marrow are all about 0.24–0.40, 0.09–0.20 and 0.033–0.050 mGy/MBq, respectively [36–38,55]. Either liver or red marrow may be the dose-limiting organ for radionuclide PEGylated nanoliposome therapy [59]. High absorbed doses are also observed in the gastrointestinal tract, including the lower

large intestine, upper large intestine and small intestine. This suggests ^{188}Re -liposome was mostly excreted via feces. Very low absorbed doses of ^{188}Re -liposome are noted in the organs of the central nervous and musculoskeletal systems. Bone marrow toxicity is also generally dose-limiting for β -emitting radiopharmaceuticals. Those results indicated the nanoliposome formulation did not cause higher absorbed doses in normal tissue than nontargeted formulation, but it did cause higher absorbed doses in tumors. Systemically targeted radionuclide therapy using ^{188}Re -liposome is feasible, promising, and may have the advantage and benefit of reduced toxicity and improved therapeutic efficacy.

4.4. Acute Toxicity of BMEDA and ^{188}Re -Liposome

Non-clinical safety studies are necessary to assess the safety and toxicity profiles of drug compounds under development and before clinical trials [60]. Acute toxicity studies in various animal models aiming to provide pharmaceutical information intended for human use, and the information is useful for providing preliminary identification of target organs of toxicity. Since BMEDA ($\text{C}_{10}\text{H}_{24}\text{N}_2\text{S}_2$) is a new chemical entity for chelating ^{188}Re in ^{188}Re -liposome, the acute toxicity studies of BMEDA should be evaluated. The LD_{50} value of BMEDA is estimated to be 8.13 and 8.68 mg/kg in rodents for male and female mice, respectively. No difference in body weights and no observable gross lesions are observed among 3- and 6-mg/kg BMEDA-treated and control mice [45]. Extended acute toxicity studies of BMEDA have also been confirmed in non-rodents, with beagles receiving a BMEDA dose of 1 mg/kg that had no adverse effect and no doses causing life-threatening toxicity [46].

A 28-day extended acute toxicity study for ^{188}Re -liposome was performed in Sprague Dawley rats via a single intravenous injection, obtaining the “no observed adverse effect level (NOAEL)” estimated to be greater than 185 MBq (5 mCi) per rat (weight of a rat estimated to be 200 g) [48]. None of the rats died and no clinical sign was observed during the 28-day study period. No differences in the biochemistry parameters, gross lesion and histopathological damage were found between the ^{188}Re -liposome treated and control groups.

4.5. Therapeutic and Combination Effects of ^{188}Re -Liposome

The treatment of colorectal cancer patients remains a challenging problem [61]. We demonstrated the therapeutic efficacy of ^{188}Re -liposome in C26 [22] or LS-174 [38] colorectal tumor bearing mice. Mice receiving various doses of ^{188}Re -liposome (from 22.2 to 37 MBq) can significantly increase overall survival time by more than 60% compared with control saline injection. The results showed the dose-dependent therapeutic efficacy and prolonged survival time of ^{188}Re -liposome in colorectal tumor-bearing mice [22,38]. Liposomal drugs such as pegylated liposomal doxorubicin (DXR) can be designed to improve the pharmacological and therapeutic index for cancer therapeutics [2,13], but the limited distribution of doxorubicin in solid tumors causes drug resistance and a lower chemotherapy response [62]. The developments for improving therapeutic efficacy, reducing side effects and overcoming the drug resistance of multiplex nanoliposomes are of considerable interest.

For the therapeutic efficacy in a C26 murine colon carcinoma solid tumor model [34], the tumor volume inhibition and the survival curves following various treatments are shown in Figure 5A,B, respectively. Two (25%) of the mice treated with ^{188}Re -DXR-liposome (Figure 5C) or ^{188}Re -liposome were completely cured after 120 days. The bimodality radio-chemotherapeutics of ^{188}Re -DXR-liposome and radiotherapeutic of ^{188}Re -liposome showed better mean growth inhibition (MGI) rates (MGI = 0.048; 74 days) and (MGI = 0.134; 60 days), respectively, than those treated with chemotherapeutics of Lipo-DOX (MGI = 0.413; 38 days) (Figure 5D). The therapeutic efficacy of ^{188}Re -liposome and the synergistic effect of the combination of ^{188}Re -DXR-liposome point to the potential benefit and promise of the co-delivery of nanoliposome radio-chemotherapeutics for adjuvant cancer treatment on oncology applications [34].

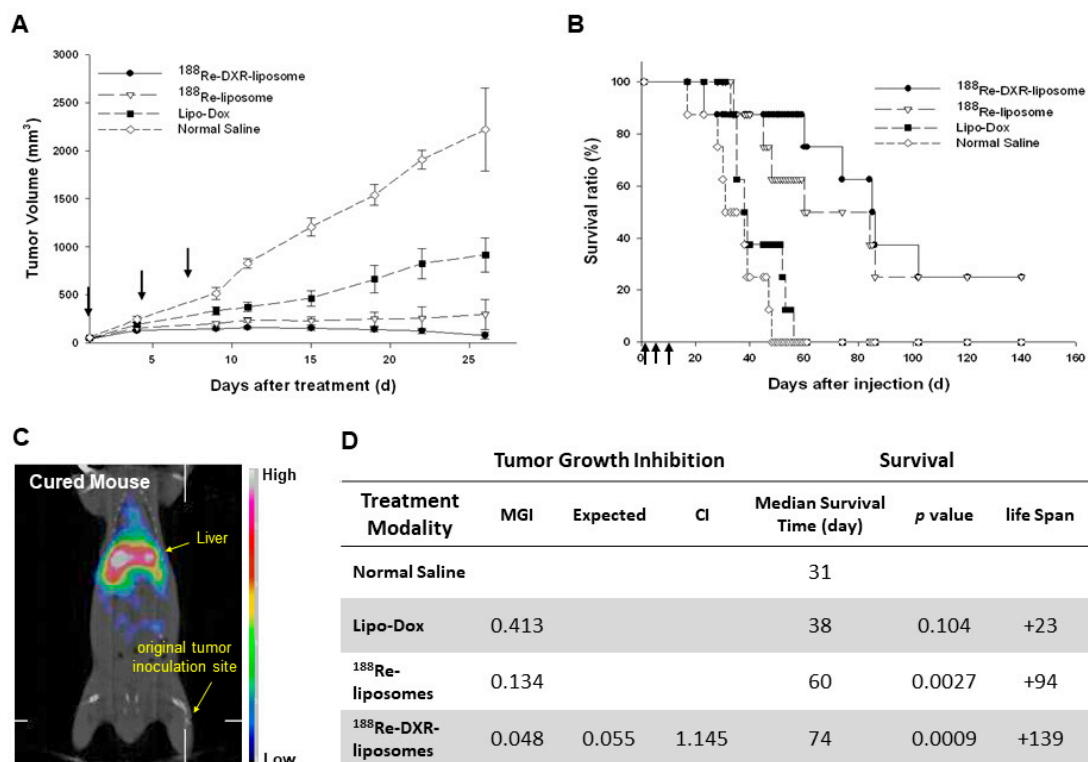


Figure 5. Tumor volume (A) and survival ratio (B) versus time following administering $^{188}\text{Re-DXR-liposome}$ (22.2 MBq of ^{188}Re and 2 mg/kg DXR) (●), $^{188}\text{Re-liposome}$ (22.2 MBq of ^{188}Re) (▽), Lipo-Dox (2 mg/kg DXR) (■) and normal saline (◇) by triple intravenous injection on Day 0, 4 and 8 in C26 murine colon tumor-bearing mice. (C) MicroSPECT/CT image of $^{188}\text{Re-DXR-liposome}$ at 120 day after treatment. (D) Statistics of therapeutic efficacy of $^{188}\text{Re-liposome}$ compared with Lipo-DOX. CI: Combination Index; MGI: Mean Growth Inhibition. Figures adapted with permission from [34].

For several decades, 5-Fluorouracil (5-FU)-based regimens have been the first choice of the primary or adjuvant chemotherapy for colorectal cancer [63,64]. We compared the therapeutic efficacy by single equivalent dose (80% maximum tolerance dose, MTD) of $^{188}\text{Re-liposome}$ (80% MTD; 29.6 MBq) with that of 5-FU (80% MTD; 144 mg/kg) in different tumor models [22,36–38]. All therapeutic results including median survival time and tumor volume inhibition demonstrated better therapeutic $^{188}\text{Re-liposome}$ efficacy (80% MTD) than that of 5-FU (80% MTD) treatment in mice. For the comparative therapeutic study of $^{188}\text{Re-liposome}$ and 5-FU in a C26 murine colon carcinoma solid tumor mice model [22], the tumor volume inhibition and the survival curves following various treatments are shown in Figure 6A,B, respectively. With respect to therapeutic efficacy, the tumor-bearing mice treated with $^{188}\text{Re-liposome}$ showed a better mean tumor growth inhibition rate (MGI) and longer median survival time (MGI = 0.140; 80 days) than those treated with the anti-cancer drug 5-FU (MGI = 0.195; 69 days) and untreated control mice (48 days) (Figure 6C).

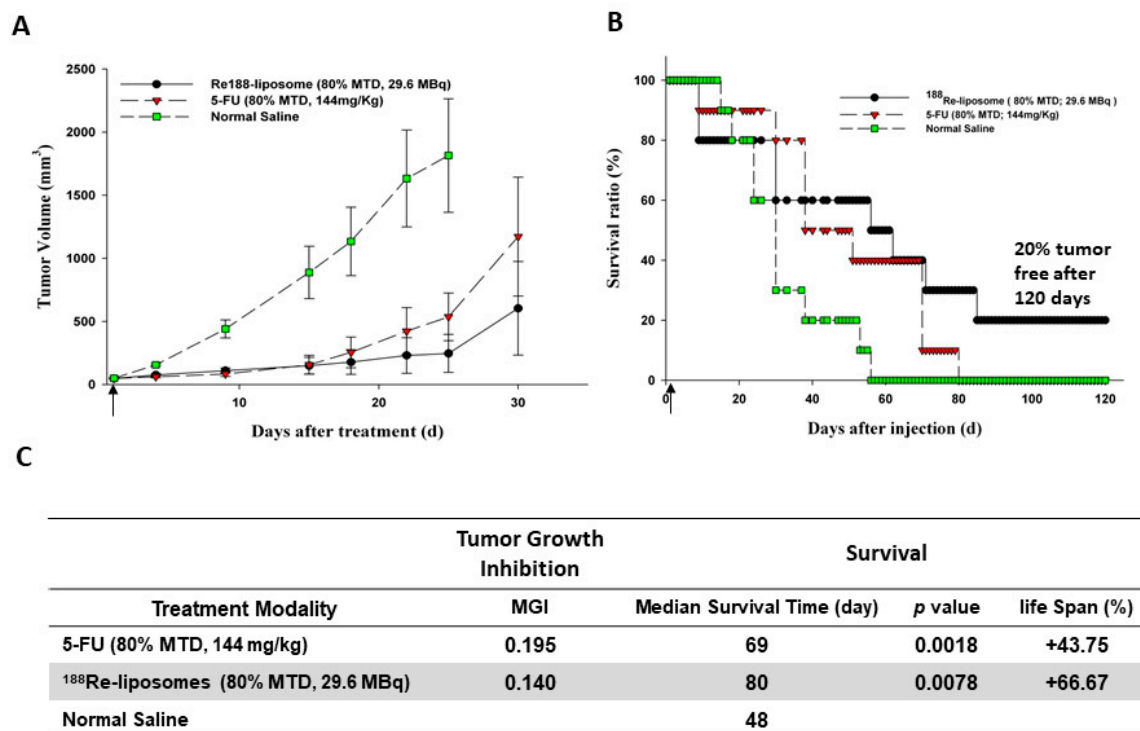


Figure 6. Tumor volume (A) and survival ratio (B) versus time following administering ^{188}Re -liposome (80% MTD, 29.6 MBq) or 5-FU (80% MTD, 144 mg/kg) by single intravenous injection in C26 murine colon tumor-bearing mice. (C) Statable ^{188}Re -liposome compared with 5-FU. Figures adapted with permission from [22].

In the comparative therapeutic study of ^{188}Re -liposome and 5-FU in a C26 murine colon peritoneal ascites and tumor mice model [36], significant inhibitions of hemorrhagic ascites formation (Figure 7A) and the inhibition of tumor growth (Figure 7B) were observed in the ^{188}Re -liposome treated group (83.3%, 63%) in comparison with the 5-FU (44.9%, 9.1%). The survival curves after various treatments were showed in Figure 7C. With respect to therapeutic efficacy, the tumor-bearing mice treated with ^{188}Re -liposome showed better mean survival time and increased life span (32.8 days, 34.6%) than those treated with the anti-cancer drug 5-FU (26.7 days, 9.6%) and untreated control mice (24.3 days) (Figure 7D).

We also worked on studies of combination therapy using ^{188}Re -liposome and chemo therapeutic agents. ^{188}Re -liposome was combined with sorafenib (Nexavar) [42], or Lipo-Dox [43] in C26 colorectal tumor mouse models. Hsu showed mice treated with ^{188}Re -liposome and Lipo-Dox pretreatment experienced limited tumor growth (Figure 8A). Seventy-five percent of the mice could survive with the combination of ^{188}Re -liposome and Lipo-Dox. Groups with Lipo-Dox or ^{188}Re -liposome treatment showed a survival rate of less than 25% at the same time point [43]. With respect to therapeutic efficacy, the tumor-bearing mice treated with ^{188}Re -liposome and pretreated with Lipo-Dox showed increased mean survival time and increased life span (more than 120 days, 242.9%) compared to those treated with ^{188}Re -liposome (57 days, 62.9%) or Lipo-Dox (47.5 days; 35.7%) and untreated control mice (35 days) (Figure 8B). ^{188}Re -liposome combined with Nexavar achieved higher survival rates (75%) compared with the ^{188}Re -liposome (62.5%) or Nexavar (0%) alone groups at the end of the study (Figure 8D) [42]. The therapeutic effect of the chemotherapeutic agent for the tumor significantly improved by ^{188}Re -liposome demonstrated its delivery and effectiveness.

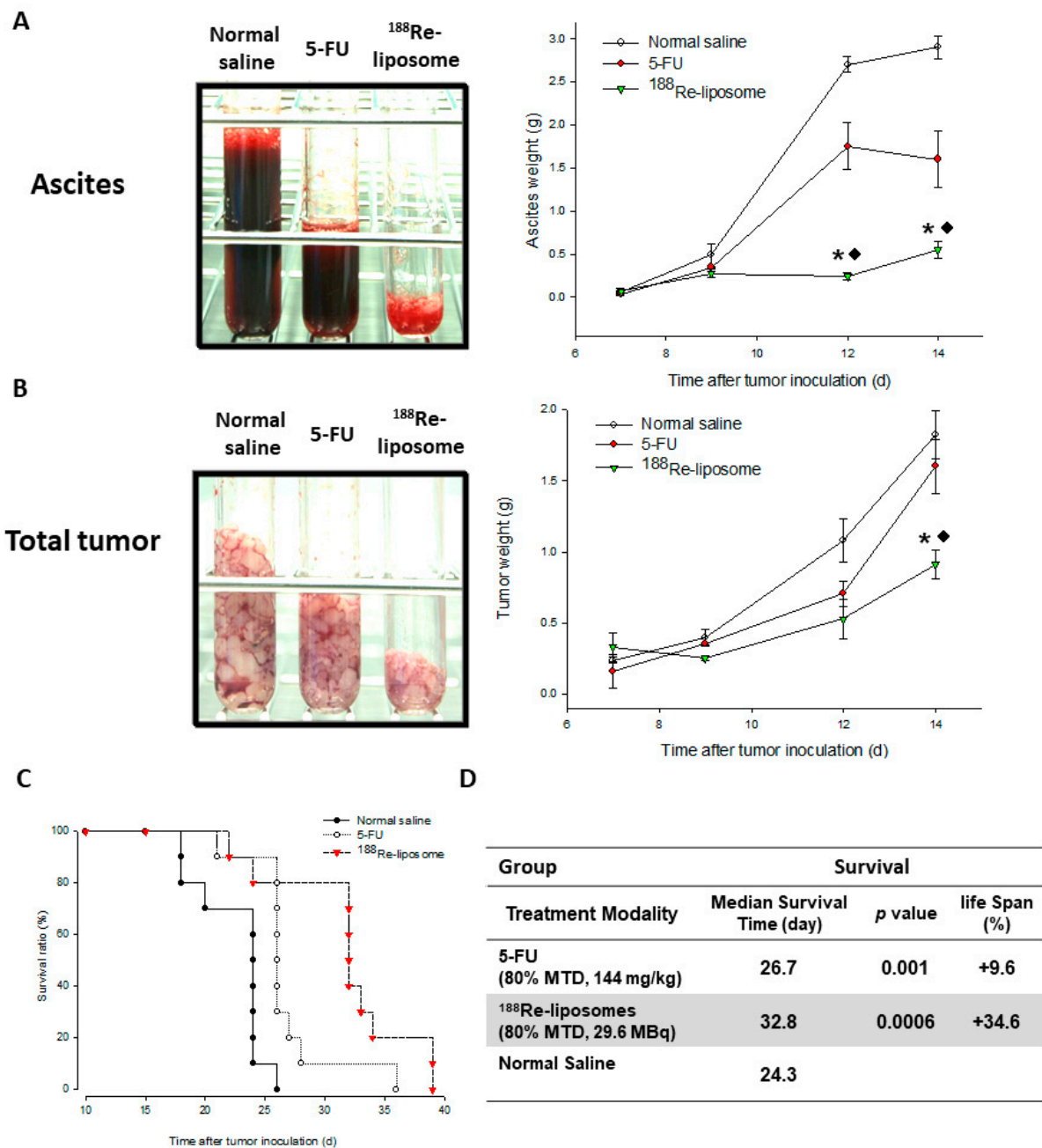


Figure 7. The total ascites weight (A), tumors weight (B) and survival ratio (C) following administering ¹⁸⁸Re-liposome (80% MTD, 29.6 MBq), 5-FU (80% MTD, 144 mg/kg), and normal saline, respectively by single intravenous injection in C26 peritoneal metastatic tumor-bearing mice. *: significant difference between ¹⁸⁸Re-liposome- and normal saline-treated groups; ♦: significant difference between ¹⁸⁸Re-liposome- and 5-FU-treated groups. (D) Statistics of therapeutic efficacy of ¹⁸⁸Re-liposome compared with 5-FU. Figures adapted with permission from [36].

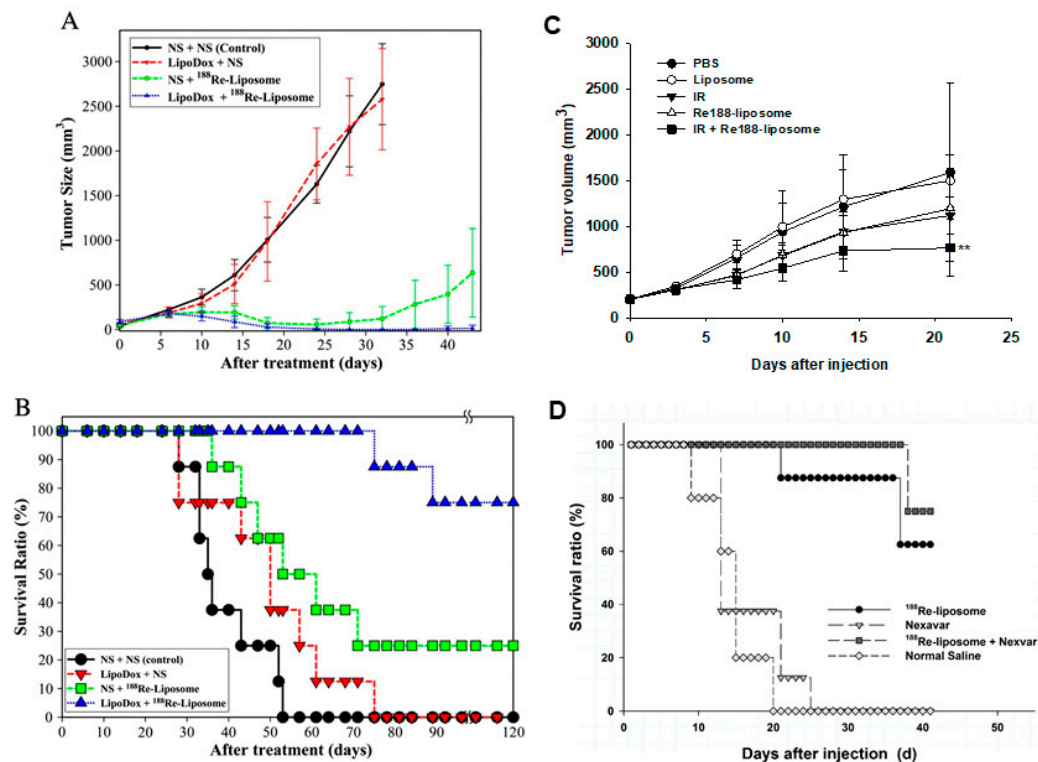


Figure 8. Combination therapy of ¹⁸⁸Re-liposome with Lipo-Dox, EBRT or Nexavar. Measurements of tumor growth (A) and survival ratio (B) in C26 tumor-bearing mice responded to a treatment regimen in which the mice were injected with either saline or Lipo-Dox (2.5 mg/kg) prior to an injection of the ¹⁸⁸Re-liposome (22.2 MBq) on day 0. (C) Therapeutic effect of EBRT and ¹⁸⁸Re-liposome. For combination treatment, BE-3 tumor-bearing mice received EBRT (IR, 3 Gy) followed by ¹⁸⁸Re-liposome (13.2 MBq). Single treatment of EBRT, ¹⁸⁸Re-liposome, liposome and normal saline were used for comparison. EBRT: external beam radiotherapy; IR: ionizing radiation. (D) Therapeutic effect of Nexavar and ¹⁸⁸Re-liposome. For combination treatment, C26-luc murine colon tumor-bearing mice received ¹⁸⁸Re-liposome (29.6 MBq) and Nexavar (10 mg/kg, once every other day for 1 week) by intrasplenic injection. ¹⁸⁸Re-liposome or Nexavar treatment only was used for comparison. Figures adapted with permission from [42–44].

External beam radiotherapy (EBRT) can deliver high-energy radiation beams to cover both gross tumors and potential microscopic tumor cells in the vicinity of a tumor, including esophageal cancers. Our studied showed ¹⁸⁸Re-liposome combined with EBRT achieved higher tumor growth inhibition (53%) compared with the ¹⁸⁸Re-liposome (25%) or EBRT (30%) alone groups at 21 days post-injection (Figure 8C) [44]. Combination treatment had no additive adverse effects or significant biological toxicities on white blood cell counts, body weight, or liver and renal functions. According to combination studies of ¹⁸⁸Re-liposome with chemotherapeutics or EBRT, the combination strategy may be a potential treatment modality for cancers.

5. Clinical Studies of ¹⁸⁸Re-Liposome

The FDA guidelines for an exploratory IND (eIND) published in 2006 [65] give the ability to conduct a human trial for obtaining early pharmacokinetic and pharmacodynamics information according to the microdosing concept. The term microdosing is defined as less than 1/100th of the dose calculated to yield a pharmacological effect of the drug candidate based on primary in vitro and in vivo data and administered at a maximum dose of ≤100 μg [24,66]. Due to the BMEDA being the first to be used in humans, the eIND is an approach to evaluate the imaging, pharmacokinetic and safety of ¹⁸⁸Re-liposome.

An open-label, single-arm, phase 0 clinical trial with a 111 MBq microdose of ¹⁸⁸Re-liposome injected in patients with metastatic cancer was carried out. The study proved the

safety of ^{188}Re -liposome in 12 patients refractory to current standard/available therapies. None of the subjects showed any serious adverse effects following ^{188}Re -liposome injection, and no clinically significant abnormalities in physical exams or laboratory exams were found [29]. Patient 14, who had a nasopharyngeal tumor (NPC) over the left nasal cavity and lung metastases, showed high uptake (3.99% IA/kg) at the targeted area at 24 h after injection with ^{188}Re -liposome, corresponding to the soft tissue lesion (blue arrow) seen on the corresponding MRI (Figure 9A,B). Anterior planar images of Patient 14 were obtained at different time points following injection with ^{188}Re -liposome and reveal a discernible uptake of radioactivity in the left nasopharyngeal region (Figure 9C). This nasopharyngeal tumor shows a clear response to the low radioactivity of ^{188}Re -liposome, as verified by nasopharyngoscopic examinations at two and twelve months after injection (Figure 9D–F) [29].

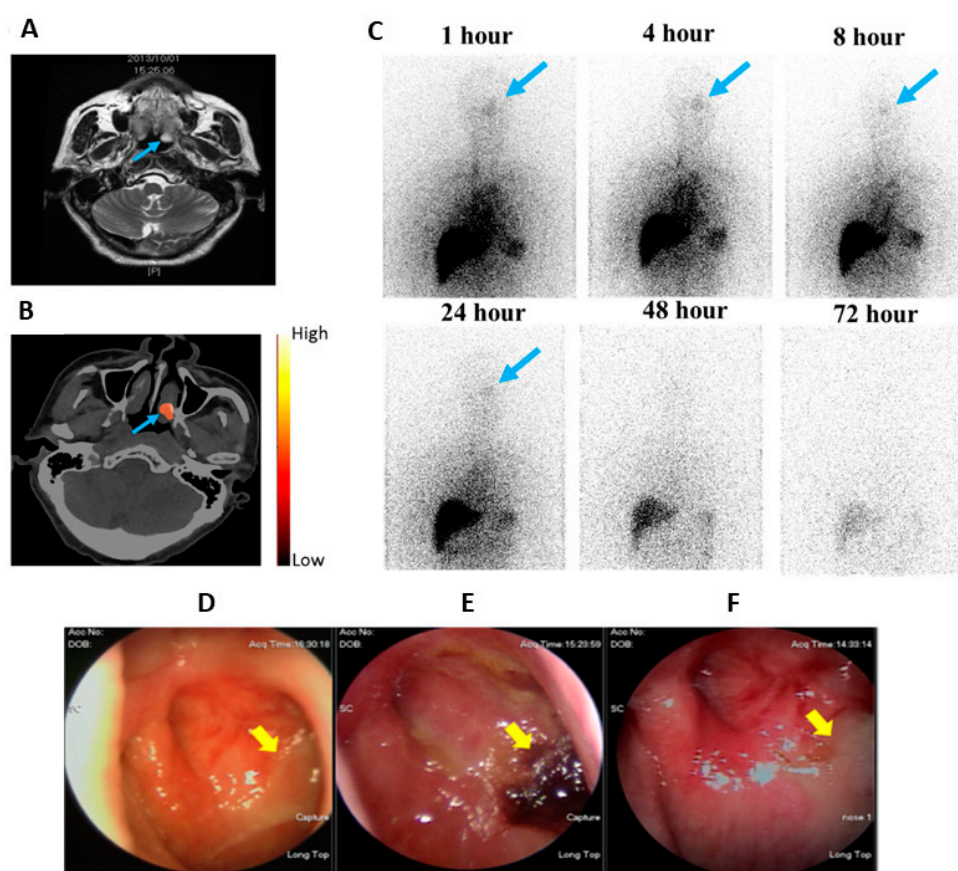


Figure 9. Phase 0 clinical studies of ^{188}Re -liposome SPECT/CT imaging showing tumor targeting and uptake in a NPC patient (Pt. 14) with pulmonary and mediastinal metastasis: (A) One month before ^{188}Re -liposome injection, MRI shows there is a soft tissue lesion (blue arrow) in the left nasopharynx, (B) SPECT/CT 24 h after ^{188}Re -liposome injection as seen on the MRI, (C) Anterior upper-body images at six different time points after ^{188}Re -liposome injection (blue arrows indicate the lesion over the left nasopharynx), (D) The nasopharyngoscopic examination one month before ^{188}Re -liposome injection shows the left nasopharyngeal mass with a crust and mucoid (yellow arrow), (E) Two months after ^{188}Re -liposome injection, there are engorged blood vessels and irregular surface over the left nasopharynx (yellow arrow) and (F) One year after the trial, the nasopharyngoscopic study shows fibrosis over the left nasopharynx (yellow arrow). Figures adapted with permission from [29].

Two recurrent ovarian cancer patients received cohort 1 therapeutic activity of ^{188}Re -liposome in phase 1 clinical trials. Four months after the treatment, the CA-125 started to decline. Chest film follow-up also showed a partial resolution of right pleural effusion [25]. These results suggest ^{188}Re -liposome may reverse from a drug resistance status to a drug sensitive status and may be a novel strategy in overcoming drug resistance in ovarian cancer. Although the two cases do not prove the therapeutic efficacy of ^{188}Re -liposome, the extended life after treatment of the two cases is more than expected.

6. Conclusions

The advantages of a longer shelf-life radionuclide generator, higher energy β -emitter for radiotherapeutics and suitable gamma ray energy and half-life for nuclear imaging provide ^{188}Re with suitable characteristics for internal radiotheranostics application. However, the main disadvantage of ^{188}Re nuclear imaging is the presence of a high-energy background signals (478 keV, 633 keV, and 829 keV), with high-energy ultra-high resolution multi-pinhole collimators being required to optimize both image quality and quantitative accuracy for ^{188}Re SPECT nuclear imaging in diagnostic applications.

The effectiveness and safety of personalized medicine involves multiple factors that contribute to cancer disease types and development, and resistance to radio/chemotherapy. We demonstrated nanoliposome is a suitable passive delivery system for ^{188}Re radionuclide in various cells and tumor animal models, which include prolonging the radioactivity of ^{188}Re in tumor sites with longer biologic half-life through EPR effects, suppressing tumor growth and increasing the survival rate in various tumor animal models. However, enhanced specificity could be further considered through active targeting nanoliposome [67–69]. Although combinational use of internal nanotargeted ^{188}Re -liposome with chemotherapy in clinical settings is still in its infancy, it has heralded the dawn of a new era in future cancer treatment through our experimental achievements in preclinical animal models investigation and radio/chemo-combination therapeutic effect and survival comparison results. Nevertheless, two issues need to be overcome in those novel therapeutic strategies' design. First, the exploration of the optimal protocol of active nanotargeted radionuclide therapy in combination with nanotargeted chemotherapy to decrease the nanotargeted drugs that accumulate in the reticuloendothelial system, such as the liver, spleen, and red marrow. Second, each cancer type possesses specific clinical characteristic properties, such as the tumor microenvironment, and invasion time periods, etc. Increasing preclinical and clinical investigated results showed the effect of radiation in terms of modulating immunity could increase its therapeutic efficacy role in systemic anti-cancer treatment [67]. Local external radiation therapy in combination with chemotherapy of tumor-triggering systemic response is described as an abscopal effect. Our systemic investigations and comparison of nanotargeted ^{188}Re -liposome pharmacology as well as the therapeutic effect in various animal models and translational clinical research results point to a new novel formulation of nanotargeted ^{188}Re -liposome combining radio/chemo/EBRT/immuno-combination therapy. This could potentially enhance the nuclear imaging quality and accuracy in addition to the systemic tumor lesions treatment effectiveness.

In conclusion, this paper provides an overview and highlights our multifunctional and multi-institutes collaboration of nanotargeted ^{188}Re -liposome from preclinical tumor and ascites animal models to preliminary clinical translation studies. The results demonstrate ^{188}Re -liposome is both capable and favorable in vivo tumor targeting and nuclear imaging, biodistribution, pharmacokinetics, dosimetry, radiotherapeutic effectiveness, and has a good synergistic radio/chemo-combination effect. However, further efforts and challenges in preclinical and clinical efficacy and toxicity studies are required to translate the new novel nanotargeted ^{188}Re -liposome with the radio/chemo/immuno-combination magic bullet therapeutic concept to further advance new technologies to clinical applications for the healthcare benefits of suitable cancer patients.

Author Contributions: Conceptualization, C.-H.C., T.-W.L. and G.T.; methodology, M.-C.C., L.-C.C. and Y.-J.C.; writing—review and editing, C.-H.C. and G.T.; supervision, T.-W.L., C.-H.C. and G.T. All authors have read and agreed to the published version of the manuscript.

Funding: Financial support was received from National Science and Technology Program for Nanoscience and Nanotechnology, National Science Council, Taiwan and Department of Industrial Technology, Ministry of Economic Affairs, Taiwan.

Institutional Review Board Statement: Not applicable.

Informed Consent Statement: Not applicable.

Data Availability Statement: Not applicable.

Conflicts of Interest: The authors declare no conflict of interest.

References

1. Filippi, L.; Chiaravallotti, A.; Schillaci, O.; Cianni, R.; Bagni, O. Theranostic approaches in nuclear medicine: Current status and future prospects. *Expert Rev. Med. Devices* **2020**, *17*, 331–343. [[CrossRef](#)] [[PubMed](#)]
2. Torchilin, V.P. Recent advances with liposomes as pharmaceutical carriers. *Nat. Rev. Drug Discov.* **2005**, *4*, 145–160. [[CrossRef](#)]
3. Filipczak, N.; Pan, J.; Yalamarty, S.S.K.; Torchilin, V.P. Recent advancements in liposome technology. *Adv. Drug Deliv. Rev.* **2020**, *156*, 4–22. [[CrossRef](#)]
4. Ting, G.; Chang, C.H.; Wang, H.E.; Lee, T.W. Nanotargeted radionuclides for cancer nuclear imaging and internal radiotherapy. *J. Biomed. Biotechnol.* **2010**, *2010*, 1–17. [[CrossRef](#)] [[PubMed](#)]
5. Terreno, E.; Uggeri, F.; Aime, S. Image guided therapy: The advent of theranostic agents. *J. Control. Release* **2012**, *161*, 328–337. [[CrossRef](#)] [[PubMed](#)]
6. Lammers, T.; Aime, S.; Hennink, W.E.; Storm, G.; Kiessling, F. Theranostic nanomedicine. *Acc. Chem. Res.* **2011**, *44*, 1029–1038. [[CrossRef](#)] [[PubMed](#)]
7. Jeon, J. Review of Therapeutic Applications of Radiolabeled Functional Nanomaterials. *Int. J. Mol. Sci.* **2019**, *20*, 2323. [[CrossRef](#)] [[PubMed](#)]
8. Man, F.; Gawne, P.J.; de Rosales, R.T. Nuclear imaging of liposomal drug delivery systems: A critical review of radiolabelling methods and applications in nanomedicine. *Adv. Drug Deliv. Rev.* **2019**, *143*, 134–160. [[CrossRef](#)] [[PubMed](#)]
9. Goins, B.; Bao, A.; Phillips, W.T. Techniques for Loading Technetium-99m and Rhenium-186/188 Radionuclides into Preformed Liposomes for Diagnostic Imaging and Radionuclide Therapy. *Methods Mol. Biol.* **2017**, *1522*, 155–178. [[CrossRef](#)]
10. Ehlerding, E.B.; Goel, S.; Cai, W. Cancer theranostics with ⁶⁴Cu/¹⁷⁷Lu-loaded liposomes. *Eur. J. Nucl. Med. Mol. Imaging* **2016**, *43*, 938–940. [[CrossRef](#)]
11. Ting, G.; Tseng, Y.L.; Chang, C.H.; Lee, T.W. Applications in diagnostics. Chapter 4: Nanotargeted radiopharmaceuticals for nuclear imaging and radiotherapy. In *Handbook of Nanobiomedical Research*; World Scientific Publishing Company: Singapore, 2014; Volume 3, pp. 77–125.
12. Ting, G.; Chang, C.H.; Wang, H.E. Cancer nanotargeted radiopharmaceuticals for tumor imaging and therapy. *Anticancer Res.* **2009**, *29*, 4107–4118.
13. Allen, T.M.; Cullis, P.R. Drug delivery systems: Entering the mainstream. *Science* **2004**, *303*, 1818–1822. [[CrossRef](#)]
14. van der Geest, T.; Laverman, P.; Metselaar, J.M.; Storm, G.; Boerman, O.C. Radionuclide imaging of liposomal drug delivery. *Expert Opin. Drug Deliv.* **2016**, *13*, 1231–1242. [[CrossRef](#)]
15. Lamichhane, N.; Udayakumar, T.S.; D'Souza, W.D.; Simone, C.B., 2nd; Raghavan, S.R.; Polf, J.; Mahmood, J. Liposomes: Clinical Applications and Potential for Image-Guided Drug Delivery. *Molecules* **2018**, *23*, 288. [[CrossRef](#)] [[PubMed](#)]
16. Harrington, K.J.; Mohammadtaghi, S.; Uster, P.S.; Glass, D.; Peters, A.M.; Vile, R.G.; Stewart, J.S. Effective targeting of solid tumors in patients with locally advanced cancers by radiolabeled pegylated liposomes. *Clin. Cancer Res.* **2001**, *7*, 243–254. [[PubMed](#)]
17. Uccelli, L.; Pasquali, M.; Boschi, A.; Giganti, M.; Duatti, A. Automated preparation of Re-188 lipiodol for the treatment of hepatocellular carcinoma. *Nucl. Med. Biol.* **2011**, *38*, 207–213. [[CrossRef](#)] [[PubMed](#)]
18. Boschi, A.; Massi, A.; Uccelli, L.; Pasquali, M.; Duatti, A. PEGylated N-methyl-S-methyl dithiocarbamate as a new reagent for the high-yield preparation of nitrido Tc-99m and Re-188 radiopharmaceuticals. *Nucl. Med. Biol.* **2010**, *37*, 927–934. [[CrossRef](#)]
19. Bao, A.; Goins, B.; Klipper, R.; Negrete, G.; Phillips, W.T. ¹⁸⁶Re-liposome labeling using ¹⁸⁶Re-SNS/S complexes: In vitro stability, imaging, and biodistribution in rats. *J. Nucl. Med.* **2003**, *44*, 1992–1999. [[PubMed](#)]
20. Wu, Q.; Allouch, A.; Martins, I.; Brenner, C.; Modjtahedi, N.; Deutsch, E.; Perfettini, J.L. Modulating Both Tumor Cell Death and Innate Immunity Is Essential for Improving Radiation Therapy Effectiveness. *Front. Immunol.* **2017**, *8*, 613. [[CrossRef](#)] [[PubMed](#)]
21. Friesen, C.; Lubatschowski, A.; Kotzerke, J.; Buchmann, I.; Reske, S.N.; Debatin, K.M. Beta-irradiation used for systemic radioimmunotherapy induces apoptosis and activates apoptosis pathways in leukaemia cells. *Eur. J. Nucl. Med. Mol. Imaging* **2003**, *30*, 1251–1261. [[CrossRef](#)] [[PubMed](#)]
22. Chang, Y.J.; Hsu, C.W.; Chang, C.H.; Lan, K.L.; Ting, G.; Lee, T.W. Therapeutic efficacy of ¹⁸⁸Re-liposome in a C26 murine colon carcinoma solid tumor model. *Investig. New Drugs* **2013**, *31*, 801–811. [[CrossRef](#)] [[PubMed](#)]

23. Shen, Y.A.; Lan, K.L.; Chang, C.H.; Lin, L.T.; He, C.L.; Chen, P.H.; Lee, T.W.; Lee, Y.J.; Chuang, C.M. Intraperitoneal ^{188}Re -Liposome delivery switches ovarian cancer metabolism from glycolysis to oxidative phosphorylation and effectively controls ovarian tumour growth in mice. *Radiother. Oncol.* **2016**, *119*, 282–290. [[CrossRef](#)] [[PubMed](#)]
24. Chang, C.Y.; Chen, C.C.; Lin, L.T.; Chang, C.H.; Chen, L.C.; Wang, H.E.; Lee, T.W.; Lee, Y.J. PEGylated liposome-encapsulated rhenium-188 radiopharmaceutical inhibits proliferation and epithelial-mesenchymal transition of human head and neck cancer cells in vivo with repeated therapy. *Cell Death Discov.* **2018**, *4*, 100. [[CrossRef](#)] [[PubMed](#)]
25. Chang, C.M.; Lan, K.L.; Huang, W.S.; Lee, Y.J.; Lee, T.W.; Chang, C.H.; Chuang, C.M. ^{188}Re -Liposome Can Induce Mitochondrial Autophagy and Reverse Drug Resistance for Ovarian Cancer: From Bench Evidence to Preliminary Clinical Proof-of-Concept. *Int. J. Mol. Sci.* **2017**, *18*, 903. [[CrossRef](#)]
26. Bartel, D.P. MicroRNAs: Genomics, biogenesis, mechanism, and function. *Cell* **2004**, *116*, 281–297. [[CrossRef](#)]
27. Lin, L.T.; Chang, C.Y.; Chang, C.H.; Wang, H.E.; Chiou, S.H.; Liu, R.S.; Lee, T.W.; Lee, Y.J. Involvement of let-7 microRNA for the therapeutic effects of Rhenium-188-embedded liposomal nanoparticles on orthotopic human head and neck cancer model. *Oncotarget* **2016**, *7*, 65782–65796. [[CrossRef](#)]
28. Lin, B.Z.; Wan, S.Y.; Lin, M.Y.; Chang, C.H.; Chen, T.W.; Yang, M.H.; Lee, Y.J. Involvement of Differentially Expressed microRNAs in the PEGylated Liposome Encapsulated ^{188}Re -Mediated Suppression of Orthotopic Hypopharyngeal Tumor. *Molecules* **2020**, *25*, 3609. [[CrossRef](#)]
29. Wang, S.J.; Huang, W.S.; Chuang, C.M.; Chang, C.H.; Lee, T.W.; Ting, G.; Chen, M.H.; Chang, P.M.; Chao, T.C.; Teng, H.W.; et al. A phase 0 study of the pharmacokinetics, biodistribution, and dosimetry of ^{188}Re -liposome in patients with metastatic tumors. *EJNMMI Res.* **2019**, *9*, 46. [[CrossRef](#)]
30. Chang, Y.J.; Chang, C.H.; Chang, T.J.; Yu, C.Y.; Chen, L.C.; Jan, M.L.; Luo, T.Y.; Lee, T.W.; Ting, G. Biodistribution, pharmacokinetics and microSPECT/CT imaging of ^{188}Re -BMEDA-liposome in a C26 murine colon carcinoma solid tumor animal model. *Anticancer Res.* **2007**, *27*, 2217–2225. [[PubMed](#)]
31. Chen, M.H.; Chang, C.H.; Chang, Y.J.; Chen, L.C.; Yu, C.Y.; Wu, Y.H.; Lee, W.C.; Yeh, C.H.; Lin, F.H.; Lee, T.W.; et al. MicroSPECT/CT imaging and pharmacokinetics of ^{188}Re -(DXR)-liposome in human colorectal adenocarcinoma-bearing mice. *Anticancer Res.* **2010**, *30*, 65–72. [[PubMed](#)]
32. Chen, L.C.; Chang, C.H.; Yu, C.Y.; Chang, Y.J.; Hsu, W.C.; Ho, C.L.; Yeh, C.H.; Luo, T.Y.; Lee, T.W.; Ting, G. Biodistribution, pharmacokinetics and imaging of ^{188}Re -BMEDA-labeled pegylated liposomes after intraperitoneal injection in a C26 colon carcinoma ascites mouse model. *Nucl. Med. Biol.* **2007**, *34*, 415–423. [[CrossRef](#)] [[PubMed](#)]
33. Huang, F.Y.; Lee, T.W.; Kao, C.H.; Chang, C.H.; Zhang, X.; Lee, W.Y.; Chen, W.J.; Wang, S.C.; Lo, J.M. Imaging, autoradiography, and biodistribution of ^{188}Re -labeled PEGylated nanoliposome in orthotopic glioma bearing rat model. *Cancer Biother. Radiopharm.* **2011**, *26*, 717–725. [[CrossRef](#)] [[PubMed](#)]
34. Chang, Y.J.; Chang, C.H.; Yu, C.Y.; Chang, T.J.; Chen, L.C.; Chen, M.H.; Lee, T.W.; Ting, G. Therapeutic efficacy and microSPECT/CT imaging of ^{188}Re -DXR-liposome in a C26 murine colon carcinoma solid tumor model. *Nucl. Med. Biol.* **2010**, *37*, 95–104. [[CrossRef](#)] [[PubMed](#)]
35. Chen, L.C.; Chang, C.H.; Yu, C.Y.; Chang, Y.J.; Wu, Y.H.; Lee, W.C.; Yeh, C.H.; Lee, T.W.; Ting, G. Pharmacokinetics, microSPECT/CT imaging and therapeutic efficacy of ^{188}Re -DXR-liposome in C26 colon carcinoma ascites mice model. *Nucl. Med. Biol.* **2008**, *35*, 883–893. [[CrossRef](#)] [[PubMed](#)]
36. Tsai, C.C.; Chang, C.H.; Chen, L.C.; Chang, Y.J.; Lan, K.L.; Wu, Y.H.; Hsu, C.W.; Liu, I.H.; Ho, C.L.; Lee, W.C.; et al. Biodistribution and pharmacokinetics of ^{188}Re -liposomes and their comparative therapeutic efficacy with 5-fluorouracil in C26 colonic peritoneal carcinomatosis mice. *Int. J. Nanomed.* **2011**, *6*, 2607–2619. [[CrossRef](#)]
37. Chen, L.C.; Wu, Y.H.; Liu, I.H.; Ho, C.L.; Lee, W.C.; Chang, C.H.; Lan, K.L.; Ting, G.; Lee, T.W.; Shien, J.H. Pharmacokinetics, dosimetry and comparative efficacy of ^{188}Re -liposome and 5-FU in a CT26-luc lung-metastatic mice model. *Nucl. Med. Biol.* **2012**, *39*, 35–43. [[CrossRef](#)]
38. Hsu, C.W.; Chang, Y.J.; Chang, C.H.; Chen, L.C.; Lan, K.L.; Ting, G.; Lee, T.W. Comparative therapeutic efficacy of rhenium-188 radiolabeled-liposome and 5-fluorouracil in LS-174T human colon carcinoma solid tumor xenografts. *Cancer Biother. Radiopharm.* **2012**, *27*, 481–489. [[CrossRef](#)]
39. Liu, C.M.; Lee, W.C.; Yu, C.Y.; Lan, K.L.; Chang, C.H.; Ting, G.; Lee, T.W. Comparison of the therapeutic efficacy of ^{188}Re -liposomes and liposomal doxorubicin in a 4T1 murine orthotopic breast cancer model. *Oncol Rep.* **2012**, *27*, 678–684. [[CrossRef](#)]
40. Lin, L.T.; Chang, C.H.; Yu, H.L.; Liu, R.S.; Wang, H.E.; Chiu, S.J.; Chen, F.D.; Lee, T.W.; Lee, Y.J. Evaluation of the therapeutic and diagnostic effects of PEGylated liposome-embedded ^{188}Re on human non-small cell lung cancer using an orthotopic small-animal model. *J. Nucl. Med.* **2014**, *55*, 1864–1870. [[CrossRef](#)]
41. Huang, F.Y.; Lee, T.W.; Chang, C.H.; Chen, L.C.; Hsu, W.H.; Chang, C.W.; Lo, J.M. Evaluation of ^{188}Re -labeled PEGylated nanoliposome as a radionuclide therapeutic agent in an orthotopic glioma-bearing rat model. *Int. J. Nanomed.* **2015**, *10*, 463–473. [[CrossRef](#)]
42. Chang, Y.J.; Hsu, W.H.; Chang, C.H.; Lan, K.L.; Ting, G.; Lee, T.W. Combined therapeutic efficacy of ^{188}Re -liposomes and sorafenib in an experimental colorectal cancer liver metastasis model by intrasplenic injection of C26-luc murine colon cancer cells. *Mol. Clin. Oncol.* **2014**, *2*, 380–384. [[CrossRef](#)] [[PubMed](#)]

43. Hsu, W.H.; Liu, S.Y.; Chang, Y.J.; Chang, C.H.; Ting, G.; Lee, T.W. The PEGylated liposomal doxorubicin improves the delivery and therapeutic efficiency of ^{188}Re -Liposome by modulating phagocytosis in C26 murine colon carcinoma tumor model. *Nucl. Med. Biol.* **2014**, *41*, 765–771. [[CrossRef](#)]
44. Chang, C.H.; Liu, S.Y.; Chi, C.W.; Yu, H.L.; Chang, T.J.; Tsai, T.H.; Lee, T.W.; Chen, Y.J. External beam radiotherapy synergizes ^{188}Re -liposome against human esophageal cancer xenograft and modulates ^{188}Re -liposome pharmacokinetics. *Int. J. Nanomed.* **2015**, *10*, 3641–3649. [[CrossRef](#)]
45. Chang, C.H.; Chiu, S.P.; Chiang, T.C.; Lee, T.W. Acute intravenous injection toxicity of BMEDA in mice. *Drug Chem. Toxicol.* **2011**, *34*, 20–24. [[CrossRef](#)]
46. Liu, S.Y.; Chang, C.H.; Lee, T.W. Single dose acute toxicity testing for N,N-bis(2-mercaptoethyl)-N',N' diethylethylenediamine in beagles. *Regul. Toxicol. Pharm.* **2014**, *69*, 217–225. [[CrossRef](#)] [[PubMed](#)]
47. Liu, C.M.; Chang, C.H.; Chang, Y.J.; Hsu, C.W.; Chen, L.C.; Chen, H.L.; Ho, C.L.; Yu, C.Y.; Chang, T.J.; Chiang, T.C.; et al. Preliminary evaluation of acute toxicity of ^{188}Re -BMEDA-liposome in rats. *J. Appl. Toxicol.* **2010**, *30*, 680–687. [[CrossRef](#)]
48. Chi-Mou, L.; Chia-Che, T.; Chia-Yu, Y.; Wan-Chi, L.; Chung-Li, H.; Tsui-Jung, C.; Chih-Hsien, C.; Te-Wei, L. Extended acute toxicity study of ^{188}Re -liposome in rats. *J. Appl. Toxicol.* **2013**, *33*, 886–893. [[CrossRef](#)] [[PubMed](#)]
49. Boschi, A.; Uccelli, L.; Pasquali, M.; Duatti, A.; Taibi, A.; Pupillo, G.; Esposito, J. $^{188}\text{W}/^{188}\text{Re}$ Generator System and Its Therapeutic Applications. *J. Chem.* **2014**, *2014*, 1–14. [[CrossRef](#)]
50. IAEA. *Production of Long Lived Parent Radionuclides for Generators: ^{68}Ge , ^{82}Sr , ^{90}Sr and ^{188}W* ; Radioisotopes and Radiopharmaceuticals Series No. 2; International Atomic Energy Agency: Vienna, Austria, 2010; pp. 80–106.
51. Lepareur, N.; Lacoueille, F.; Bouvry, C.; Hindre, F.; Garcion, E.; Cherel, M.; Noiret, N.; Garin, E.; Knapp, F.F.R., Jr. Rhenium-188 Labeled Radiopharmaceuticals: Current Clinical Applications in Oncology and Promising Perspectives. *Front. Med.* **2019**, *6*, 132. [[CrossRef](#)] [[PubMed](#)]
52. Wang, S.J.; Lin, W.Y.; Chen, M.N.; Hsieh, B.T.; Shen, L.H.; Tsai, Z.T.; Ting, G.; Knapp, F.F., Jr. Radiolabelling of Lipiodol with generator-produced ^{188}Re for hepatic tumor therapy. *Appl. Radiat. Isot.* **1996**, *47*, 267–271. [[CrossRef](#)]
53. Ni, H.C.; Yu, C.Y.; Chen, S.J.; Chen, L.C.; Lin, C.H.; Lee, W.C.; Chuang, C.H.; Ho, C.L.; Chang, C.H.; Lee, T.W. Preparation and imaging of rhenium-188 labeled human serum albumin microsphere in orthotopic hepatoma rats. *Appl. Radiat. Isot.* **2015**, *99*, 117–121. [[CrossRef](#)] [[PubMed](#)]
54. Chen, L.C.; Chang, Y.J.; Chen, S.J.; Lee, W.C.; Chang, C.H.; Lee, T.W.; Shien, J.H. Imaging, biodistribution and efficacy evaluation of ^{188}Re -human serum albumin microspheres via intraarterial route in an orthotopic hepatoma model. *Int. J. Radiat. Biol.* **2017**, *93*, 477–486. [[CrossRef](#)]
55. Chang, C.H.; Stabin, M.G.; Chang, Y.J.; Chen, L.C.; Chen, M.H.; Chang, T.J.; Lee, T.W.; Ting, G. Comparative dosimetric evaluation of nanotargeted ^{188}Re -DXR-liposome for internal radiotherapy. *Cancer Biother. Radiopharm.* **2008**, *23*, 749–758. [[CrossRef](#)] [[PubMed](#)]
56. Sgouros, G. Dosimetry of internal emitters. *J. Nucl. Med.* **2005**, *46*, 18S–27S. [[PubMed](#)]
57. Coulam, C.H.; Lee, J.H.; Wedding, K.L.; Spielman, D.M.; Pelc, N.J.; Kee, S.T.; Hill, B.B.; Bouley, D.M.; Derby, G.C.; Myers, B.D.; et al. Noninvasive measurement of extraction fraction and single-kidney glomerular filtration rate with MR imaging in swine with surgically created renal arterial stenoses. *Radiology* **2002**, *223*, 76–82. [[CrossRef](#)]
58. Stabin, M.G.; Sparks, R.B.; Crowe, E. OLINDA/EXM: The second-generation personal computer software for internal dose assessment in nuclear medicine. *J. Nucl. Med.* **2005**, *46*, 1023–1027. [[PubMed](#)]
59. Emfietzoglou, D.; Kostarelos, K.; Sgouros, G. An analytic dosimetry study for the use of radionuclide-liposome conjugates in internal radiotherapy. *J. Nucl. Med.* **2001**, *42*, 499–504.
60. Marzin, D. Preclinical evaluation of radiopharmaceutical toxicological prerequisites. *Nucl. Med. Biol.* **1998**, *25*, 733–736. [[CrossRef](#)]
61. Gallagher, D.J.; Kemeny, N. Metastatic colorectal cancer: From improved survival to potential cure. *Oncology* **2010**, *78*, 237–248. [[CrossRef](#)] [[PubMed](#)]
62. Wolpin, B.M.; Meyerhardt, J.A.; Mamon, H.J.; Mayer, R.J. Adjuvant treatment of colorectal cancer. *CA Cancer J. Clin.* **2007**, *57*, 168–185. [[CrossRef](#)]
63. Hegde, S.R.; Sun, W.; Lynch, J.P. Systemic and targeted therapy for advanced colon cancer. *Expert Rev. Gastroenterol. Hepatol.* **2008**, *2*, 135–149. [[CrossRef](#)]
64. Wolpin, B.M.; Mayer, R.J. Systemic treatment of colorectal cancer. *Gastroenterology* **2008**, *134*, 1296–1310. [[CrossRef](#)]
65. Food and Drug Administration. *Guidance for Industry, Investigators, and Reviewers. Exploratory IND Studies*; Food and Drug Administration: Rockville, MD, USA, 2006.
66. Matson, M.L.; Villa, C.H.; Ananta, J.S.; Law, J.J.; Scheinberg, D.A.; Wilson, L.J. Encapsulation of alpha-Particle-Emitting $^{225}\text{Ac}^{3+}$ Ions Within Carbon Nanotubes. *J. Nucl. Med.* **2015**, *56*, 897–900. [[CrossRef](#)]
67. Hsu, W.C.; Cheng, C.N.; Lee, T.W.; Hwang, J.J. Cytotoxic Effects of PEGylated Anti-EGFR Immunoliposomes Combined with Doxorubicin and Rhenium-188 Against Cancer Cells. *Anticancer Res.* **2015**, *35*, 4777–4788. [[PubMed](#)]
68. Huang, Y.S.; Hsu, W.C.; Lin, C.H.; Lo, S.N.; Cheng, C.N.; Lin, M.S.; Lee, T.W.; Chang, C.H.; Lan, K.L. Bi-Functional Radiotheranostics of ^{188}Re -Liposome-Fcy-hEGF for Radio- and Chemo-Therapy of EGFR-Overexpressing Cancer Cells. *Int. J. Mol. Sci.* **2021**, *22*, 1902. [[CrossRef](#)] [[PubMed](#)]
69. Liu, S.Y.; Lo, S.N.; Lee, W.C.; Hsu, W.C.; Lee, T.W.; Chang, C.H. Evaluation of Nanotargeted ^{111}In -Cyclic RGDfK-Liposome in a Human Melanoma Xenotransplantation Model. *Int. J. Mol. Sci.* **2021**, *22*, 1099. [[CrossRef](#)] [[PubMed](#)]